ChemPubSoc Europe

DOI: 10.1002/cbic.201200659

Caged CO_2 for the Direct Observation of CO_2-Consuming Reactions

Katharina Lommel,[a] Gabriela Schäfer,[a] Konstantin Grenader,[b] Christoph Ruland,[a] Andreas Terfort,[b] Werner Mäntele,[a] and Georg Wille*[a]

CO_2-consuming reactions, in particular carboxylations, play important roles in technical processes and in nature. Their kinetic behavior and the reaction mechanisms of carboxylating enzymes are difficult to study because CO_2 is inconvenient to handle as a gas, exists in equilibrium with bicarbonate in aqueous solution, and typically yields products that show no significant spectroscopic differences from the reactants in the UV/Vis range. Here we demonstrate the utility of 3-nitrophenylacetic acid and related compounds (caged CO_2) in conjunction with infrared spectroscopy as widely applicable tools for the investigation of such reactions, permitting convenient measurement of the kinetics of CO_2 consumption. The use of isotopically labeled caged CO_2 provides a tool for the assignment of infrared absorption bands, thus aiding insight into reaction intermediates and mechanisms.

Introduction

CO_2-consuming reactions are very common and important both in the chemical industry and in nature. Moreover, technical Carbon Capture and Storage (CCS) has been discussed as one way to reduce atmospheric CO_2,[1] but the biological pathway is even more important: ribulose-1,5-bisphosphate-carboxylase/oxygenase (RuBisCO), the CO_2-fixing enzyme in photosynthesis, is the most abundant enzyme on earth, providing the major pathway for removing CO_2 from the atmosphere.[2] Many other carboxylating enzymes play crucial roles in the metabolism of all organisms;[3] examples include the biotin-dependent enzymes involved in fatty acid synthesis (acetyl-coenzyme A carboxylase) and gluconeogenesis (pyruvate carboxylase), the carbamoylphosphate synthase of the urea cycle, and the CO_2-fixing phosphoenolpyruvate carboxylase (PEPC).

Despite their importance and ubiquity, CO_2-utilizing enzymes are generally difficult to study. UV–visible spectroscopy, a standard tool in enzyme kinetics, often fails because the reactants (CO_2 or bicarbonate and an organic compound) and the products (the carboxylated compound) rarely exhibit distinct spectral features in the UV–visible region. As a result, activity assays described in the literature are often discontinuous (employing radioactive $^{14}CO_2$, for example), or use helper enzymes in coupled reactions, precluding the observation of fast processes. Furthermore, CO_2—being a gas under "biochemical" conditions—is tedious to handle. The rapid and well-defined concentration jumps required for the observation of pre-steady-state kinetics or enzyme-bound intermediates are especially difficult to generate. Bicarbonate, which exists in a pH-dependent equilibrium with CO_2 in aqueous solution, can be used as a substitute, although the two species clearly differ chemically, and enzymes usually accept only one of the two as substrate. We show here a way to tackle these problems by combining IR spectroscopy with the use of photodecarboxylating compounds.

IR spectroscopy, however, is ideally suited for the observation of CO_2: in aqueous solution the molecule exhibits a very strong IR absorbance band (absorption coefficient $\varepsilon = 1.5 \times 10^6\ cm^2\,mol^{-1}$) at 2343 cm^{-1};[4] that is, in a spectral region without overlap from signals of other, specifically biochemically relevant, compounds. Furthermore, the absorbance band of CO_2 in aqueous solution lacks the typical substructure from rotational transitions that would be visible in the gas phase, so dissolved and atmospheric CO_2 can easily be distinguished. IR spectroscopy has been used previously in an activity assay for a decarboxylating enzyme[5] and also for the observation of an enzyme-bound CO_2 species in the active site of carbonic anhydrase.[6]

The second component of our approach—photoactivatable or caged compounds—are established tools for the rapid generation of concentration jumps by flash photolysis and subsequent observation of chemical reactions.[7–13] Many of these reagents release CO_2 in addition to their intended effector molecule, either as a result of their mechanism of effector release (e.g., in the amine-yielding photolysis of carbamates[14,15]) or in undesired side-reactions that limit the cage's efficiency.[16,17]

Nitrophenylacetic acids and their anions have been shown to decarboxylate quickly and efficiently upon irradiation with UV light,[18] and their good solubilities and stabilities have made them attractive candidates for use as caged CO_2 com-

[a] K. Lommel,[+] Dr. G. Schäfer,[+] C. Ruland, Prof. Dr. W. Mäntele, Dr. G. Wille
Institut für Biophysik, Johann Wolfgang Goethe-Universität Frankfurt
Max-von-Laue-Str. 1, 60438 Frankfurt am Main (Germany)
E-mail: wille@biophysik.uni-frankfurt.de

[b] K. Grenader, Prof. Dr. A. Terfort
Institut für Anorganische und Analytische Chemie
Johann Wolfgang Goethe-Universität Frankfurt
Max-von-Laue-Str. 7, 60438 Frankfurt am Main (Germany)

[+] These authors contributed equally to this work.

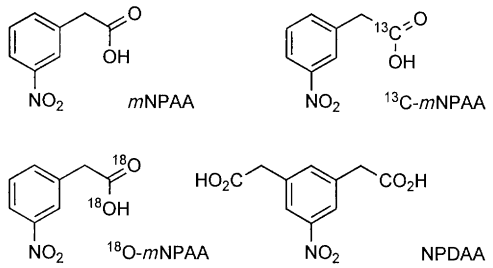

Scheme 1. Caged CO_2 compounds investigated in this study.

pounds. Their mechanisms of photolysis have recently been studied in exquisite detail, both theoretically and experimentally.[19,20] In particular, 3-nitrophenylacetic acid (*m*NPAA, Scheme 1) shows promise as caged CO_2. It is a small molecule that decarboxylates very rapidly and efficiently ($\tau \approx 200$ ps, quantum yield 0.63), releasing just CO_2 and one other, inert side product (3-nitrotoluene). The very fast reaction is a prerequisite for time-resolved IR measurements because any intramolecular reactions of the caged compound will be finished before the first spectrum is acquired after photolysis. The simplicity of the reaction also helps in the IR band assignment.

To facilitate the identification of CO_2-associated bands in the IR spectra, we also synthesized the isotopically labeled derivatives 2-(3-nitrophenyl)(1-^{13}C)acetic acid (^{13}C-*m*NPAA) and 2-(3-nitrophenyl)($^{18}O_2$)acetic acid (^{18}O-*m*NPAA). Furthermore, 2,2′-(5-nitro-1,3-phenylene)diacetic acid (NPDAA) was prepared, with the aim of generating two moles of CO_2 per mole of cage, thereby reducing the amount of the poorly soluble side product.

Results and Discussion

Synthesis of derivatives

The synthesis of the 3-nitrophenylacetic acids started from 1-(chloromethyl)-3-nitrobenzene via the corresponding nitriles (obtained with KCN or K^{13}CN), which were then hydrolyzed with H_2O or $H_2{}^{18}O$. The diacid NPDAA was prepared in a similar fashion by starting from 5-nitroisophthalic acid via the alcohol and the corresponding bromomethyl derivatives. Mass spectra and ^{1}H and ^{13}C NMR spectra confirmed the structures of the products. The mass spectral analysis of ^{18}O-*m*NPAA showed that ^{18}O-labeling was not complete, most likely due to exposure of the substance to acidic aqueous conditions during the final extraction. It is known that in aqueous solutions carboxylic acids exchange carbonyl oxygen atoms with the solvent.[21]

Photolysis of caged CO_2 compounds

Solutions of all compounds were photolyzed by use of a UV light pulse (308 nm, ≈20 ns, 220 mJ pulse energy) from a XeCl excimer laser. Although the absorbance of *m*NPAA at 308 nm is only ≈25% of that at the maximum at 270 nm,[19] the use of this wavelength avoids excessive absorption by proteins in the sample. Figure 1 shows the difference spectra obtained in each

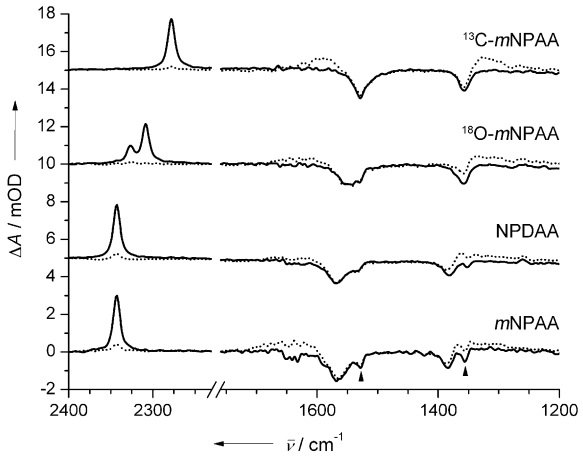

Figure 1. Difference FTIR spectra of the four compounds. The concentration of each compound is 20 mM in 100 mM sodium phosphate buffer (pH 7.3), 295 K. Spectra were normalized to equal integral absorbance of the CO_2 peak near 2300 cm^{-1} to account for small differences in optical path length or flash intensities. ——: "5 s after photolysis" minus "before photolysis"; ····: "120 s after photolysis" minus "before photolysis". The spectra are stacked on the absorbance scale to avoid overlap. Arrows indicate the symmetric and antisymmetric $-NO_2$ stretching bands.

case by subtracting the IR spectrum before the laser flash from the spectrum obtained 5 s after light exposure.

m*NPAA*: The prominent peak at 2343 cm^{-1} results from the antisymmetric stretching vibration of CO_2 physically dissolved in water. The rotational structure that would be visible in the spectrum of gaseous CO_2 is absent. One set of negative bands is associated with the loss of carboxylate, as expected (ν_{as} = 1565 cm^{-1}, ν_s = 1381 cm^{-1}). The other two negative bands are most likely due to a small reduction in the absorption coefficient of the aromatic nitro group upon decarboxylation (ν_{as} = 1537 cm^{-1}, ν_s = 1355 cm^{-1}). Under the experimental conditions, a peak height at 2343 cm^{-1} of 3 mOD corresponds to a CO_2 concentration of 4 mM: that is, effective photolysis of 20% of the total cage in the sample. This agrees with the observation that a second flash on the same sample produced a very similar "after-minus-before" difference spectrum (not shown) with an integrated CO_2 peak area of about 75% of the first one. The photolytic efficiency might be somewhat underestimated due to the fact that some CO_2 will have reacted with water before the first IR spectrum is obtained (see below).

NPDAA: The photoinduced difference spectrum of the diacid is very similar to that of *m*NPAA. For equal peak areas of CO_2, the peaks associated with the nitro group (arrows in Figure 1) are smaller by about 40%. The effect indicates that under the experimental conditions used here [flash duration (≈20 ns) > photochemical relaxation ($\tau \approx 200$ ps in *m*NPAA)], two molecules of CO_2 are indeed released from at least a proportion of the cage molecules. From a mechanistic standpoint, it would be intriguing to look at the decarboxylation of this diacid on the ultrafast time scale and with theoretical approaches. In particular, it would be interesting to see whether both carboxylates can be cleaved simultaneously from the excited state. This, however, would require ultrafast spectroscopic techniques

and much shorter laser pulses, and was not the focus of the present study.

^{18}O-mNPAA: Two effects are immediately apparent. Heterogeneous labeling of the cage compound, as indicated by mass spectrometry, yields both $C^{18}O_2$ (2309 cm^{-1}) and $C^{16}O^{18}O$ (2327 cm^{-1}) in a ratio of ≈80:20. $C^{16}O_2$ is initially almost completely absent. Also, the corresponding carboxylate peaks are downshifted, so that one of them coincides with the nitro group peak at 1358 cm^{-1}, whereas the other carboxylate peak at 1557 cm^{-1} almost coincides with the second nitro group peak at 1540 cm^{-1}.

^{13}C-mNPAA: $^{13}CO_2$ exhibits an isotope effect on the frequency of the antisymmetric CO_2 stretching vibration that is even larger than for $C^{18}O_2$: the band is shifted towards 2278 cm^{-1}. The corresponding carboxylate peaks are also further downshifted and now coincide with those of the nitro group (1358 cm^{-1}, 1529 cm^{-1}).

Under the experimental conditions, in particular at pH 7.3, the released CO_2 will react with water to form bicarbonate via carbonic acid. The end point of the reaction after 120 s is also shown in Figure 1. Bicarbonate causes very broad bands with maxima around 1650 cm^{-1} (1600 cm^{-1} for $H^{13}CO_3^-$) and 1360 cm^{-1} (1330 cm^{-1} for $H^{13}CO_3^-$).

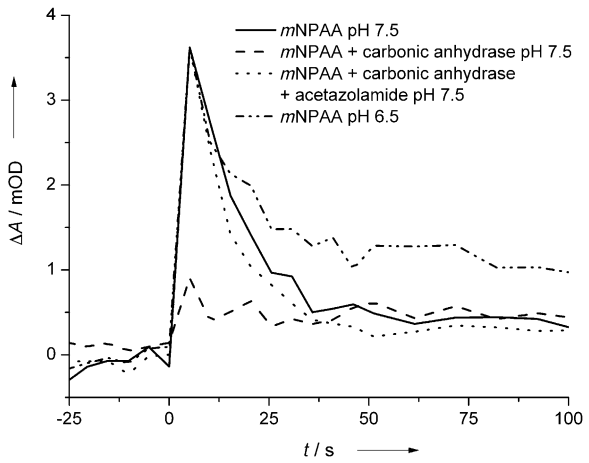

Figure 2. Reaction behavior of photolytically released CO_2 ($t = 0$ s) under different conditions (100 mM Na-HEPES buffer, 295 K), monitored at 2343 cm^{-1}. Except for the measurement with uninhibited carbonic anhydrase, curves were scaled to match with that of *m*NPAA at pH 7.5 without additives, to account for small variations in optical path length and pulse intensity in the different samples.

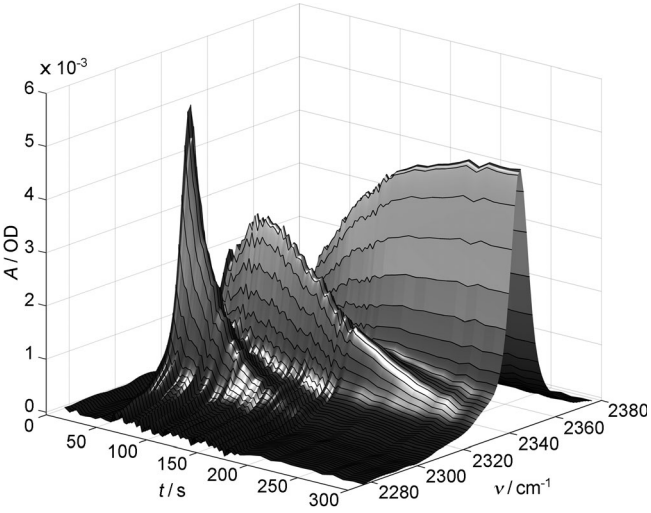

Figure 3. Time course of isotope exchange of $C^{18}O_2$ after photolytic release from ^{18}O-*m*NPAA: 50 mM ^{18}O-*m*NPAA in 100 mM phosphate buffer, pH 5.5, 293 K was flashed after baseline acquisition (at 51.2 s).

Hydration of CO_2

After its photolytic release from the caged compounds, CO_2 will re-equilibrate in water, forming bicarbonate via carbonic acid. At pH 7.5 as used here, the main pathway is the reaction between CO_2 and water, not hydroxide, so only the equilibrium concentrations, and not the equilibration rate, will depend on pH. The new equilibrium concentration of CO_2 at pH 6.5 will thus be higher than that at pH 7.5, but the equilibrium will be attained at the same rate.

This can be clearly seen in Figure 2. Exponential fits of the decay curves in all cases yield an observed pseudo first-order rate constant of $k = 0.077\ s^{-1}$ ($\tau = 13$ s). The literature gives a value of 0.043 s^{-1} (25 °C),[22] which is in quite good agreement with the number we found, considering that no efforts were made to correct for the contribution of the reverse reaction or a likely catalytic effect of the buffer.

In many organisms hydration of CO_2 is greatly accelerated by the action of carbonic anhydrase.[23] This effect can be clearly seen in Figure 2: upon addition of 200 μg mL^{-1} of carbonic anhydrase ($c = 7$ μM) to the sample, the equilibrium is reached before the first spectrum could be obtained, but the final equilibrium level of CO_2 is the same as before. When acetazolamide, an inhibitor of carbonic anhydrase,[23] was also added (20 μM), the effect of the enzyme was suppressed, as would be expected.

A demonstration for the reaction between CO_2 and water is given in Figure 3. ^{18}O-*m*NPAA was photolyzed at acidic pH (100 mM phosphate buffer pH 5.5 in $H_2{}^{16}O$), so only a small fraction of the released CO_2 would have been converted to bicarbonate in the final equilibrium. Nevertheless, continuing reaction with water leads to the disappearance of $C^{18}O_2$ via the mixed $C^{18}O^{16}O$ intermediate, finally resulting in close to 100% $C^{16}O_2$.

Reactions between CO_2 and amines

Reactions between CO_2 and amines are of great technical importance because they represent the major method by which CO_2 is selectively removed from exhaust gases. From the resulting carbamates, CO_2 can be recovered in a concentrated form and processed further.[1] The formation of carbamates is also important in enzyme catalysis in, for example, the formation of the functioning active sites in RuBisCO,[24] urease,[25] and structurally related enzymes, the reaction mechanisms of biotin-dependent enzymes,[26] or the regulation of hemoglobin

activity.[27] We therefore investigated the reaction behavior of photolytically released CO_2 with a primary, a secondary, and a tertiary amine: ethanolamine (EA), *N*-ethyl-aminoethanol (EAE), and *N*,*N*-diethyl-aminoethanol (DEAE). The primary and secondary amines should yield carbamates under the chosen reaction conditions, whereas the tertiary amine, lacking the ability to deprotonate at the nitrogen atom after nucleophilic attack on CO_2, should not. Figure 4 shows the results. The photodecarboxylation of *m*NPAA is unaffected even in the presence of 500 mM amine, as can be seen from the prominent negative carboxylate bands and also the CO_2 peak in the case of DEAE.

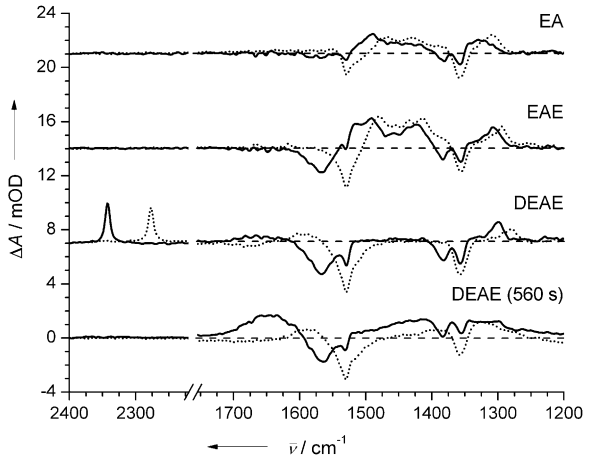

Figure 4. Reactions between amines and photolytically released CO_2. Spectra were obtained during the 5 s immediately following photolysis (500 mM amine, 200 mM sodium borate/HCl buffer, pH 9.2, 275 K). ——: mNPAA, ····: ^{13}C-mNPAA. The spectra are stacked on the absorbance scale to avoid overlap.

Both the primary and the secondary amine react with the released CO_2 on a timescale that is too fast for our experimental setup. Even at a maximum time resolution of 50 ms no trace of any CO_2 peak could be detected (not shown). If we conservatively estimate that in the noisier individual spectra obtainable after 50 ms we would be able to detect a CO_2 peak if it were more than 5% of the originally released $\approx$4 mM CO_2, we obtain a lower limit for the bimolecular rate constant of carbamate formation of 0.12 $m^3 mol^{-1} s^{-1}$. This is in agreement with literature data for the reaction between ethanolamine and CO_2 in aqueous solution—1.5 $m^3 mol^{-1} s^{-1}$ (277 K).[28]

Precise assignment of the product peaks in the region between 1800–1200 cm^{-1} to their corresponding molecular vibrations is very challenging. Even though the formation of carbamate seems fairly simple, there are accompanying side reactions that all contribute to the IR difference signal. These include formation of bicarbonate and carbonate, amine protonation, buffer response, and the formation of hydrogen bonds with the solvent. Furthermore, the hydroxy groups of the amino alcohols chosen here were shown—at least in a theoretical study—to form intramolecular hydrogen bonds with the carbamates.[29] At the very least, we can conclude that positive product peaks appear especially are particularly evident in the spectral region between 1520 and 1420 cm^{-1}. This is a clear difference from the photolysis of the cage alone, which gives no signal in this spectral region. Most of these bands shift upon isotopic replacement of $^{12}CO_2$ with $^{13}CO_2$, and must therefore involve vibrational contributions from the CO_2-derived carbon atom.

In the case of the tertiary amine the CO_2 peaks are clearly visible, unlike in the cases of the primary and secondary amines. These peaks also decay, albeit slowly, with a rate constant of $\approx$0.14 s^{-1}, due to the reaction between CO_2, water, and hydroxide under the basic conditions (pH 9.2) in the sample. However, they are accompanied not by distinct positive product bands between 1520 and 1420 cm^{-1}, but rather only by the very broad bands of bicarbonate around 1650 and 1360 cm^{-1} in a result very similar to those seen in the spectra obtained from the cage alone (Figure 1).

Binding of CO_2 to RuBisCO

One application for the caged CO_2 is the investigation of carboxylating enzymes. We first investigated the basic process of CO_2 binding to the active site of RuBisCO. Even though CO_2 is the carboxylating reagent of ribulose-1,5-bisphosphate during turnover, one extra molecule of CO_2 is first required for the generation of a fully functional active site. It carboxylates a conserved lysine residue to form a carbamate, which then acts as a binding ligand for a magnesium ion that is required for activity.[24,30–32] We set out to observe this process of initial CO_2-binding directly, and investigated the reaction behavior of photolytically released CO_2 in the presence of two different RuBisCO species and one control protein—bovine serum albumin (BSA). The last of these should not show any specific reactivity towards CO_2.

For RuBisCO from *Spinacea oleracea* (spinach, SoRuBisCO) the purification procedure we used yields an enzyme that has only 1% of the activity of the fully activated enzyme, due to the lack of carbamate in the active site.[33] In fact, the standard coupled activity assay of SoRuBisCO shows a distinct lag phase in the NADH consumption, indicating that the bicarbonate in the activity assay first has to activate the enzyme before substrate turnover can start. Recombinant RuBisCO from *Rhodospirillum rubrum* (RrRuBisCO), on the other hand, produced linear NADH consumption plots without any lag phase in the same assay, meaning either that the activation in this case is so fast that it cannot be observed during the activity assay, or that the enzyme has its carbamate already in place due to more favorable binding equilibrium constants. These two possibilities cannot be distinguished easily by this assay because the activating agent, CO_2, is also the substrate of the subsequent reaction.

In the IR measurements with photolytically released CO_2, both BSA and RrRuBisCO yielded results very similar to those seen with the cage alone: the initially high IR absorbance of photolytically released CO_2 slowly decreased until equilibrium was reached (Figure 5). This implies that the RrRuBisCO must indeed already have a fully functioning active site with a carbamate in place, as indicated by the absence of a lag phase in

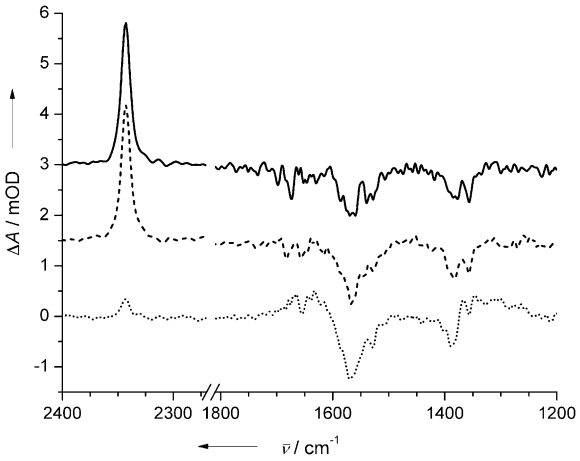

Figure 5. Reaction behavior of CO_2 in the presence of different proteins 5 s after photolytic CO_2 release (20 mM *m*NPAA, 100 mM HEPES, pH 7.5, 280 K, protein concentrations: ——: BSA 150 mg mL^{-1}, -----: RrRuBisCO 220 mg mL^{-1}, 4.1 mM active sites; ····: SoRuBisCO 150 mg mL^{-1}, 2.2 mM active sites). The spectra are stacked on the absorbance scale to avoid overlap.

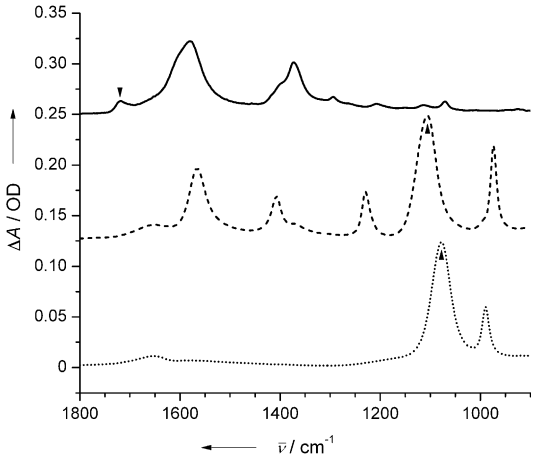

Figure 6. Stacked infrared spectra of the substrate (-----: phosphoenolpyruvate) and the products (····: phosphate and ——: oxaloacetate) of TspPEPC (100 mM in aqueous solution, pH 8.5, water background subtracted). Arrow positions indicate the wavenumbers used for kinetic observations.

the activity assay. The behavior would then be no different from that in the case of BSA.

In contrast, in the sample with SoRuBisCO the re-equilibration was too fast to be observed with the experimental setup. The resulting IR spectrum shows only the broad bicarbonate bands around 1650 and 1360 cm^{-1}. Unexpectedly, no carbamate-associated bands between 1520 and 1420 cm^{-1} are visible above noise level (compare Figure 4). The reason for this is unclear. Contamination of the preparation with carbonic anhydrase is unlikely because the results are the same in the presence of 50 μM of the carbonic anhydrase inhibitor acetazolamide (not shown).[34] A possible explanation would be an intrinsic carbonic anhydrase-like activity of SoRuBisCO, which, to the best of our knowledge, has not been described before. We note, though, that the protein concentrations typically employed in the study of SoRuBisCO are much lower than those we used here (2.2 mM of active sites), which would make the effect easy to overlook. Definite confirmation of a carbonic-anhydrase-like activity of SoRuBisCO requires further investigation.

Reaction between CO_2 and phosphoenolpyruvate carboxylase

To demonstrate the possibility of observing enzymatic turnover with the caged CO_2, we chose phosphoenolpyruvate carboxylase (PEPC). This enzyme catalyzes the primary CO_2 fixation in the photosynthetic pathways of C_4 plants and Crassulaceae and in certain microorganisms provides oxaloacetate for the citric acid cycle through an anaplerotic reaction.[35] For our purposes, it has the advantage that substrates and products are conveniently distinguishable by characteristic infrared spectral features (Figure 6).

We recombinantly expressed PEPC from *Thermus* sp. (TspPEPC) in *E. coli*.[36] The photolytic release of CO_2 starts the reaction, which can be monitored at wavelengths characteristic for each reaction partner (Figure 7). In the same assay with 0.01 mg mL^{-1} carbonic anhydrase, the reaction is complete within the dead time of the instrument, due to the high TspPEPC concentration (not shown). This shows that TspPEPC uses bicarbonate rather than CO_2 as its substrate, which is in accordance with the literature.[35] Without carbonic anhydrase, the observed reaction rates are limited by the hydration of CO_2.

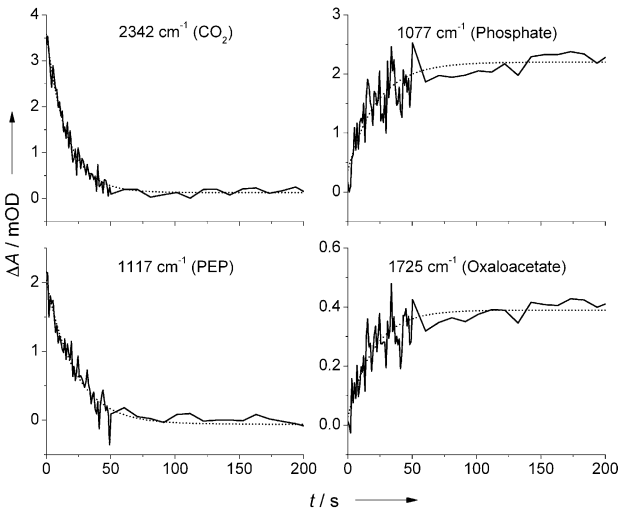

Figure 7. Time courses for four components in a reaction mixture containing 0.1 M HEPES/HCl, pH 8.5, 10 mM $MgCl_2$, 20 mM potassium phosphoenolpyruvate, 0.2 mM acetyl-coenzyme A, and 14 mg mL^{-1} TspPEPC. Dotted lines: single exponential fits.

Conclusions

In this study we have demonstrated that photodecarboxylating reagents ("caged CO_2") are indeed useful tools for the investigation of reactions involving carbon dioxide. They allow us to obtain shifts of the CO_2 concentration in solution on the nano-

second timescale. Because, immediately after photolysis, the system is far from the slow CO_2/bicarbonate equilibrium, much higher CO_2 concentrations can be reached over a wide pH range than by the more usual application of bicarbonate. If, on the other hand, the photolytically triggered, fast release of bicarbonate is desired, carbonic anhydrase can be added to the sample to accelerate the hydration of the CO_2.

Once CO_2 has been released, the course of its reactions can be easily monitored by IR spectroscopy. Its antisymmetric stretching vibration yields an intense signal at 2343 cm^{-1}: that is, in a part of the IR spectrum where only very few other compounds contribute. IR bands associated with reaction products can also be monitored, although here the precise assignment to species and vibrational modes is more difficult. As a tool for this assignment, the isotopically labeled variants of *m*NPAA presented here should be very useful. Quantum chemical approaches can also be considered for calculating normal modes and guiding IR band assignment.

The very fast photolysis of the compounds that we used as caged CO_2 should permit the study of reactions on the nanosecond timescale. With current FTIR technology we are able to observe the kinetics of reactions with time constants of $\approx$20 ms, permitting the observation of CO_2 hydration or enzyme-catalyzed product formation if the enzyme concentration is sufficiently low. Here the caged CO_2 can be applied in a universal activity assay for carboxylating enzymes.

Further technical developments should open up new possibilities for the direct observation of even faster reactions. In particular, the advent of new tunable quantum cascade lasers as intense IR light sources should allow the observation of very fast reaction kinetics at specific and variable wavelengths.

Our approach could even be applied to the direct spectroscopic observation of enzyme-bound reaction intermediates. For that purpose, the enzyme concentration must be very high to yield a sufficiently strong IR signal, and substrate consumption would therefore normally be very rapid. There are still several possible means to observe otherwise short-lived species: the reaction can be carried out at a lower temperature where turnover is slow. In this case, enzymes from thermophilic organisms can be used advantageously. Reaction intermediates can also be trapped kinetically, for example, if a second substrate that is required for turnover is omitted from the sample. Finally, genetically engineered enzyme variants that are blocked at certain reactions steps could allow the accumulation of reaction intermediates.

Experimental Section

Flash photolysis and rapid-scan FTIR spectroscopy: Rapid-scan FTIR spectra were recorded with a modified IFS 66 spectrometer (Bruker Optik, Ettlingen) and HgCdTe detector. Samples were prepared in CaF_2 cuvettes with a nominal optical path length of 5 μm and mounted in a temperature-controlled sample holder. Photolysis was induced with a XeCl excimer laser pulse at 308 nm focused on the sample ($t \approx 20$ ns, Q = 220 mJ, Model RD-EXC-200, Radiant Dyes Laser & Accessories GmbH, Wermelskirchen). The pulse was triggered by use of the spectrometer software OPUS and synchronized with IR spectrum acquisition. IR spectra were obtained in rapid-scan mode with an acquisition rate of 180 kHz and a spectral resolution of 4 cm^{-1}. The Fourier transform was carried out with Blackman–Harris three-term apodization and a zero-filling factor of two.

Static FTIR spectroscopy: Static FTIR absorption spectra of TspPEPC substrates and products were recorded with an Alpha spectrometer (Bruker Optik, Ettlingen), fitted with an in-house built ATR unit,[37] with water as background. Spectra were calculated from the averages of 128 scans with 2 cm^{-1} spectral resolution by Fourier transformation with the inbuilt parameters.

Protein purification: Bovine serum albumin and carbonic anhydrase from bovine erythrocytes were purchased from Sigma–Aldrich Chemie GmbH (Munich) and used without further purification.

SoRuBisCO: RuBisCO from *S. oleracea* was purified from fresh spinach obtained from the local supermarket with a modified procedure based on that described by Salvucci et al.[33] Instead of a Mono-Q column for anion exchange chromatography, we used a Q-Sepharose Fast Flow column (GE Healthcare, Munich). No activation through addition of bicarbonate was carried out after the purification, and buffer exchange with Amicon centrifugation devices was also carried out without added bicarbonate.

RrRuBisCO: RuBisCO from *R. rubrum* was produced by heterologous expression in *E. coli* and by a modified procedure based on that by Somerville.[38] The gene for the protein was ordered in a proprietary plasmid conferring ampicillin resistance from Mr. Gene GmbH (Regensburg) based on the amino acid sequence of UniProt entry Q2RRP5. The gene was under the control of a T7 promoter, and its codon usage had been optimized for expression in *E. coli*. Competent cells of *E. coli* strain BL21(DE3) were transformed with this plasmid and grown in terrific broth (TB) up to an OD_{600} of $\approx$0.8. Expression of the RrRuBisCO gene was induced by addition of isopropyl β-D-1-thiogalactopyranoside (IPTG, final concentration 0.5 mM) and incubation at 37 °C overnight. Harvested cells were disrupted by sonication or in a bead mill, and particulate matter was removed from the lysate by ultracentrifugation (140000 *g*, 45 min). The supernatant was removed, and protamine sulfate was added to a final concentration of 0.3% (*w/v*) from a 3% (*w/v*) stock solution. The precipitate was removed by ultracentrifugation (100000 *g*, 15 min). The supernatant was brought to 50 °C for 10 min in a water bath and then cooled on ice. The precipitate was again removed by ultracentrifugation (100000 *g*, 15 min), the supernatant was applied to a Q-Sepharose fast flow column (GE Healthcare) equilibrated with buffer [Tris·HCl (pH 8, 50 mM), $MgCl_2$ (50 mM)], dithiothreitol (DTT, 1 mM), and the protein was eluted with a rising NaCl gradient in the same buffer (0–400 mM NaCl, three column volumes). RrRuBisCO-containing fractions (as judged by an SDS-PAGE gel) were pooled, concentrated to a final volume of 3 mL, applied to a Sephacryl S75 column (GE Healthcare, Munich) equilibrated with buffer [HEPES (pH 7.5, 20 mM), NaCl (100 mM)], and eluted with the same buffer. Again, the RrRuBisCO-containing fractions were pooled and diluted to a final conductivity of <1 mS cm^{-1}. The protein was then applied to a Source Q column (GE Healthcare, Munich) equilibrated with buffer [HEPES (pH 7.5, 20 mM)] and eluted with a rising NaCl gradient in the same buffer (0–300 mM NaCl, five column volumes). RrRuBisCO-containing fractions were pooled, concentrated, and frozen at −70 °C until use.

TspPEPC: TspPEPC from *T.* sp. was produced by heterologous expression in *E. coli*. The gene for the protein was ordered in a proprietary plasmid conferring ampicillin resistance from Mr. Gene, based

on the amino acid sequence of UniProt entry P51060. The gene was under the control of a T7 promoter, and its codon usage had been optimized for expression in *E. coli*. Competent cells of *E. coli* strain BL21(DE3) were transformed with this plasmid and grown overnight in medium (500 mL). Cell were harvested, washed in M9 medium, and used to inoculate 10 L of M9 medium. Cells were grown up to an OD_{600} of $\approx$0.8. Expression of the TspPEPC gene was induced by addition of IPTG (final concentration 0.2 mM) and incubation at room temperature overnight. Harvested cells were resuspended in buffer [Tris·HCl (pH 8, 50 mM), DTT (1 mM), ethylenediaminetetraacetic acid (EDTA, 1 mM)] and disrupted by sonication. Particulate matter was removed from the lysate by ultracentrifugation (140 000 *g*, 45 min). The supernatant was removed and $(NH_4)_2SO_4$ (40%, *w/v*) was added. The precipitate was collected by centrifugation. The pellet was dissolved in buffer [Tris·HCl (pH 8, 50 mM), DTT (1 mM), EDTA (1 mM)], dialyzed against this buffer (2× 2 L) overnight, and centrifuged again to remove insoluble protein. The supernatant was applied to a Q-Sepharose fast flow column (GE Healthcare) equilibrated with buffer [Tris·HCl (pH 8, 50 mM), DTT (1 mM), EDTA (1 mM)], and the protein was eluted with a rising NaCl gradient in the same buffer (0–500 mM NaCl, three column volumes). TspPEPC-containing fractions (as judged by an SDS-PAGE gel) were pooled, concentrated to a final volume of 3 mL, applied to a Sephacryl S100 column (GE Healthcare) equilibrated with buffer [Tris·HCl (pH 8, 50 mM), NaCl (150 mM)], and eluted with the same buffer. TspPEPC-containing fractions were pooled, concentrated, and frozen at −70 °C until use.

For use in the FTIR measurements, protein samples were buffer-exchanged and concentrated with Amicon centrifugation devices and the buffer specific for the measurements, which also contained the caged compound.

RuBisCO activity assays: RuBisCO activity was tested with a modified method based on that of Norton et al. in a Hitachi U-2000 spectrophotometer.[39] To avoid primary amines that might interfere with carbamate formation, we used 4-(2-hydroxyethyl)piperazine-1-ethanesulfonic acid (HEPES, pK_a 7.5) as a buffer instead of tris(hydroxymethyl)aminomethane (Tris).

TspPEPC activity assay: TspPEPC activity was tested in a modified coupled assay with malate dehydrogenase[40] in the following mixture: Tris acetate (pH 8.5, 0.1 M), $KHCO_3$ (10 mM), $MgSO_4$ (10 mM), potassium phosphoenolpyruvate (2 mM), acetyl-coenzyme A (0.2 mM) as an allosteric activator, NADH (0.1 mM), malate dehydrogenase (5 IU), TspPEPC (0.1–0.2 mg mL^{-1}). The oxidation of NADH to NAD was followed with a Hitachi U-2000 spectrophotometer. To avoid primary amines that might interfere with carbamate formation, we used HEPES (pK_a 7.5) as a buffer instead of Tris for the IR measurements.

Syntheses

General: Unless otherwise noted, all reagents were obtained commercially and used without further purification. Solvents for chromatography were technical grade and distilled prior to use. Solvents for reactions were purchased as reagent grade and distilled prior to use. Analytical TLC was performed on Macherey–Nagel Polygram SIL G/UV_{254} precoated plastic sheets for TLC, and visualization was achieved by irradiation with UV light. Column chromatography was performed with silica gel (Merck 60, particle size 0.040–0.063 mm). Solvent mixture ratios are understood as volume/volume. ^{1}H NMR and ^{13}C NMR spectra were recorded with Bruker AM 250/AV 300 instruments in $CDCl_3$/[D_6]DMSO. ESI-MS/MALDI-TOF mass spectra were obtained with a VG Platform II instrument with a Quadrupol Analyzer and a VG Tofspec instrument (Fisons), respectively. IR spectra were recorded with a Nicolet 6700 FTIR spectrometer. Melting points were determined with a "Dr. Tottoli apparatus" (Buchi Corporation) without correction.

*2-(3-Nitrophenyl)[1-^{13}C]acetonitrile (**1**)*: K^{13}CN (0.42 g, 6.24 mmol) was added to a solution of 1-(chloromethyl)-3-nitrobenzene (1.00 g, 5.85 mmol) and [18]crown-6 (0.15 g, 0.57 mmol) in acetonitrile (10 cm^3), and the bluish suspension was stirred for 24 h at 25 °C. Methylene dichloride (25 cm^3) was then added, and the now brownish suspension was filtered. The filtrate was washed with water (2×25 cm^3), dried ($MgSO_4$), and concentrated under reduced pressure to afford a brownish oil, which was used in the following step without further purification.

*2-(3-Nitrophenyl)[1-^{13}C]acetic acid (**2**, ^{13}C-m*NPAA, Scheme 1)*: A solution of crude **1** in half-concentrated HCl (20 cm^3) was heated to 100 °C for 18 h. After the system had cooled down, ethyl acetate (20 cm^3) was added, and the mixture was basified with aqueous NaOH. The resulting combined aqueous extracts were acidified with aqueous HCl and extracted with methylene dichloride. The combined organic layers were dried over $MgSO_4$ and concentrated to afford product **2** (0.46 g, 45%) as a slightly brownish solid. ^{1}H NMR ($CDCl_3$, 250 MHz): δ = 8.15–8.18 (m, 2H), 7.62–7.65 (m, 1H), 7.49–7.56 (m, 1H), 3.79 ppm (d, J = 8.0 Hz, 1H); ^{13}C NMR ($CDCl_3$, 250 MHz): δ = 176.29, 135.80, 135.15, 129.73, 124.67, 122.72, 116.65, 40.44 ppm (d, J = 55.7 Hz).

*2-(3-Nitrophenyl)acetonitrile (**3**)*: Potassium cyanide (3.8 g, 57.1 mmol) was added to a solution of 1-(chloromethyl)-3-nitrobenzene (10.0 g, 58.5 mmol) and [18]crown-6 (1.5 g, 5.7 mmol) in acetonitrile (100 cm^3), and the greenish suspension was stirred for 18 h at 25 °C. Methylene dichloride (50 cm^3) was then added, and the now brownish suspension was filtered. The filtrate was washed with water (2×50 cm^3), dried ($MgSO_4$), and concentrated under reduced pressure to yield a brownish oil, which was fractionally distilled in vacuo to afford product **3** (4.4 g, 48%) as a yellowish oil, containing [18]crown-6 (6%). ^{1}H NMR ($CDCl_3$, 250 MHz): δ = 8.21–8.23 (m, 2H), 7.71–7.74 (m, 1H), 7.57–7.64 (m, 1H), 3.89 ppm (s, 2H).

*2-(3-Nitrophenyl)[^{18}O]acetic acid (**4**, ^{18}O-m*NPAA, Scheme 1)*: A solution of **3** (0.30 g) in $H_2{}^{18}O$ (1 cm^3) in a screw-cap vial was exposed to a stream of gaseous HCl for 2 h until the solution solidified. The vial was sealed and heated for 24 h to 100 °C. After the system had cooled down, ethyl acetate was added, and the mixture was basified with aqueous NaOH. The resulting combined aqueous extracts were acidified with aqueous HCl and extracted with methylene dichloride. The combined organic layers were concentrated under reduced pressure to afford **4** (0.4 g, 114%) as a slightly brownish solid still containing some water. ^{1}H NMR ($CDCl_3$, 250 MHz): δ = 8.16–8.18 (m, 2H), 7.62–7.65 (m, 1H), 7.49–7.56 (m, 1H), 3.79 ppm (d, J = 8.0 Hz, 1H); MS (ES−): *m/z* (%): 135.4 (100), 181.6 (6.8) [M−H]$^-$ ^{18}O/^{16}O, 183.7 (17.6), [M−H]$^-$ ^{18}O/^{18}O.

*(5-Nitro-1,3-phenylene)dimethanol (**5**)*: A solution of 5-nitroisophthalic acid (4.3 g, 20.4 mmol) in tetrahydrofuran (25 cm^3) was cooled to 0 °C, and borane-tetrahydrofuran (1 N, 100 cm^3, 100 mmol) was added dropwise over 1 h. The mixture was allowed to warm up slowly to 25 °C and stirred for 36 h. Methanol (20 cm^3) was added slowly, and the mixture was filtered and concentrated. The residue was dissolved in ethyl acetate (30 cm^3), washed with water (2× 15 cm^3), dried ($MgSO_4$), filtered, and concentrated to afford the known compound **5** (3.6 g,98%) as a yellow solid, which was used in the following step without further purification. ^{1}H NMR ($CDCl_3$, 250 MHz): δ = 8.15 (s, 2H), 7.72 (s, 1H), 4.82 ppm (s, 4H) was in line with the literature.[41]

*1,3-Bis(bromomethyl)-5-nitrobenzene (**6**)*: Phosphorus tribromide (1.9 cm^3, 20 mmol) was added dropwise to a solution of crude **5** in benzene (60 cm^3). The mixture was stirred for 30 min at 25 °C and then heated to reflux for 2.5 h. After cooling down, the mixture was poured onto ice and extracted with diethyl ether (2×15 cm^3). The combined organic extracts were then washed with water (20 cm^3) and brine (20 cm^3), dried ($MgSO_4$), filtered, and concentrated under reduced pressure to afford the product **6** (5.8 g, 94%) as a slightly yellowish solid, which was used in the following step without further purification. ^{1}H NMR ($CDCl_3$, 250 MHz): $\delta = 8.19$ (s, 2H), 7.75 (s, 1H), 4.52 ppm (s, 4H) was in line with the literature.[42]

*2,2′-(5-Nitro-1,3-phenylene)diacetonitrile (**7**)*: [18]Crown-6 (0.18 g, 0.67 mmol), KCN (0.49 g, 7.36 mmol), water (3.2 cm^3), and a small amount of KI were added at room temperature to a solution of **6** (1.03 g, 3.35 mmol) in acetonitrile (40 mL). After having been stirred for 72 h, the reaction mixture was worked up with water and ethyl acetate. The combined organic extracts were washed with brine, dried ($MgSO_4$), and concentrated under reduced pressure. Column chromatography (SiO_2) of the residue with hexane/ethyl acetate as the eluent provided **7** (0.47 g, 59%) as a yellowish solid. M.p. 110–112 °C; ^{1}H NMR ($CDCl_3$, 250 MHz): $\delta = 8.22$ (s, 2H), 7.72 (s, 1H), 3.92 ppm (s, 4H); ^{13}C NMR ($CDCl_3$, 250 MHz): $\delta =$ 147.42, 133.47, 133.37, 123.11, 116.16, 23.60 ppm; IR (ATR): $\tilde{\nu} =$ 3073.95, 3041.51, 2954.50, 2925.33, 2324.25, 2257.48, 1782.36, 1745.31, 1623.88, 1532.37, 1464.76, 1440.71, 1409.91, 1346.95, 1321.31, 1308.39, 1238.25, 1213.66, 1157.27, 1102.96, 1013.54, 996.43, 951.90, 927.58, 898.32, 853.15, 784.55, 741.64, 664.19, 656.29 cm^{-1}; MS (ES−): *m/z*: 199.9 $[M-H]^-$; elemental analysis calcd (%) for $C_{10}H_7N_3O_2$: C 59.70, H 3.51, N 20.89; found: C 59.76, H 3.42, N 21.12.

Crystals of this compound were obtained as colorless blocks by slow evaporation of a $CDCl_3$ solution. Crystal data for **7** were obtained with a STOE IPDS-II diffractometer and graphite-monochromated $Mo_{K\alpha}$ radiation. The structures were solved by direct methods by use of the program SHELXS[43] and refined with full-matrix, least-squares on F2 with use of the program SHELXL-97.[44]

CCDC 850844 contains the supplementary crystallographic data for this paper. These data can be obtained free of charge from the Cambridge Crystallographic Data Centre via http://www.ccdc.cam.ac.uk/data_request/cif.

Crystal data for 7: Triclinic, $C_{10}H_7N_3O_2$, space group $P\bar{1}$ with $a =$ 8.0125(10) Å, $b = 8.0705(10)$ Å, $c = 8.8205(11)$ Å, $V = 461.43(10)$ Å^3, $Z = 2$, $\rho_{calcd} = 1.448$ mg m^{-13}, $\mu = 0.105$ mm^{-1}, and $F(000) = 208$. Crystal size: 0.37×0.36×0.34 mm^3. Independent reflections: 1717 with $R_{int} = 0.0303$. The structure was solved by direct methods (SHELXS-97) and refined by use of full-matrix, least-squares difference Fourier techniques. The final agreement factors are $R^1 = 0.0333$ and $wR^2 = 0.0936$ [$I > 2\sigma(I)$].

As can be seen in Figure 8, the molecule is approximately planar. The planarity is disturbed by a slight twist of the CH_2CN substituents: C(4)-C(3)-C(7)-C(8) = 171.69(10)° and C(4)-C(5)-C(9)-C(10) = 176.16(10)°. The unit cell consists of two molecules interconvertible through an inversion center. The molecules form layers consisting of staggered chain-like structures along [010]: the distance between the molecules in a chain-like structure amounts to 2.629 Å ($d_{O2\cdots H4}$), and the distance between chain-like structures to 9.810 Å ($d_{N1\cdots N1'}$). The layers are oriented parallel to (101) and alternate likewise through an inversion center accordant to the $P\bar{1}$ space group. The layer distance amounts to 3.619 Å.

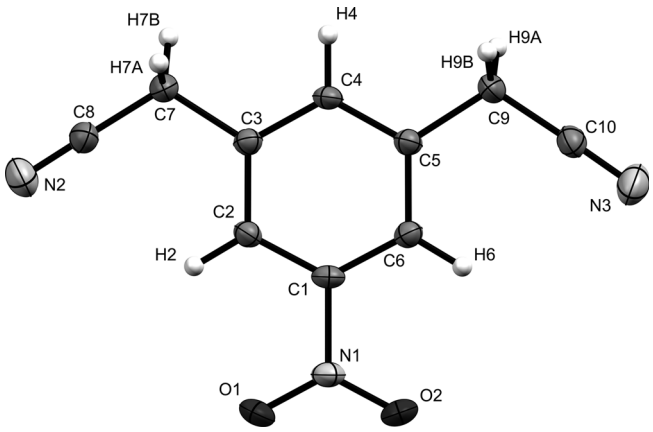

Figure 8. Single-crystal structure of **7**. Displacement ellipsoids are drawn at 50% probability level. Nitrile group bond lengths amount to 1.1392(16) Å ($d_{N2\cdots C8}$) and 1.1394(16) Å ($d_{N3\cdots C10}$), in line with the literature.[45]

*2,2′-(5-Nitro-1,3-phenylene)diacetic acid (**8**, NPDAA, Scheme 1)*: Half-concentrated HCl (20 cm^3) was added to **7** (0.45 g, 2.24 mmol), and the solution was heated to reflux for 16 h. After the system had cooled down, ethyl acetate was added, and the mixture was basified with aqueous NaOH. The resulting combined aqueous extracts were acidified with aqueous HCl and extracted with ethyl acetate. The combined organic layers were dried ($MgSO_4$) and concentrated under reduced pressure to afford **8** (0.52 g, 97%) as a slightly yellowish solid. M.p. decomposition at 203–204 °C; ^{1}H NMR ([D$_6$]DMSO, 300 MHz): $\delta = 12.51$ (br s, 1H), 8.06 (s, 2H), 7.62 (s, 1H), 3.77 ppm (s, 4H); ^{13}C NMR ([D$_6$]DMSO, 300 MHz): $\delta = 171.99$, 147.58, 137.53, 137.08, 122.65, 39.64 ppm; IR (ATR): $\tilde{\nu} = 2897.43$, 1691.10, 1536.90, 1444.82, 1415.72, 1346.62, 1300.76, 1275.75, 1254.05, 1226.63, 1184.04, 1147.21, 1100.20, 982.91, 915.81, 875.43, 813.14, 765.03, 744.59, 723.08, 668.75 cm^{-1}; MS (MALDI-TOF): *m/z*: 262.836 $[M+Na]^+$, 278.969 $[M+K]^+$.

Acknowledgements

The authors thank Hans-Werner Müller for excellent technical assistance, Fabian Dornuf for help with measurements, Prof. Alexander Heckel for advice, and the Adolf-Messer-Foundation and the "Förderfonds" of the Goethe University Frankfurt for financial support.

Keywords: caged CO_2 · carboxylation · enzyme catalysis · IR spectroscopy · photolysis

[1] Working Group III of the IPCC in *IPCC Special Report on Carbon Dioxide Capture and Storage* (Eds.: B. Metz, O. Davidson, H. de Coninck, M. Loos, L. Meyer), Cambridge University Press, Cambridge, **2005**.
[2] R. J. Ellis, *Trends Biochem. Sci.* **1979**, *4*, 241–244.
[3] S. M. Glueck, S. Gümüs, W. M. F. Fabian, K. Faber, *Chem. Soc. Rev.* **2010**, *39*, 313–328.
[4] M. Falk, A. G. Miller, *Vib. Spectrosc.* **1992**, *4*, 105–108.
[5] M. Muthusamy, M. R. Burrell, R. N. F. Thorneley, S. Bornemann, *Biochemistry* **2006**, *45*, 10667–10673.
[6] M. E. Riepe, J. H. Wang, *J. Biol. Chem.* **1968**, *243*, 2779–2787.
[7] A. P. Pelliccioli, J. Wirz, *Photochem. Photobiol. Sci.* **2002**, *1*, 441–458.
[8] A. Barth in *Dynamic Studies in Biology—Phototriggers, Photoswitches and Caged Biomolecules* (Eds.: M. Goeldner, R. Givens), Wiley-VCH, Weinheim, **2005**, pp. 369–399.

[9] G. C. R. Ellis-Davies, *Nat. Methods* **2007**, *4*, 619 – 628.
[10] G. Mayer, A. Heckel, *Angew. Chem.* **2006**, *118*, 5020 – 5042; *Angew. Chem. Int. Ed.* **2006**, *45*, 4900 – 4921.
[11] H.-M. Lee, D. R. Larson, D. S. Lawrence, *ACS Chem. Biol.* **2009**, *4*, 409 – 427.
[12] C. Brieke, F. Rohrbach, A. Gottschalk, G. Mayer, A. Heckel, *Angew. Chem.* **2012**, *124*, 8572 – 8604; *Angew. Chem. Int. Ed.* **2012**, *51*, 8446 – 8476.
[13] W. Mäntele, *Trends Biochem. Sci.* **1993**, *18*, 197 – 202.
[14] G. Papageorgiou, J. E. T. Corrie, *Tetrahedron* **1997**, *53*, 3917 – 3932.
[15] G. Papageorgiou, A. Barth, J. E. T. Corrie, *Photochem. Photobiol. Sci.* **2005**, *4*, 216 – 220.
[16] A. Barth, S. R. Martin, J. E. T. Corrie, *Photochem. Photobiol. Sci.* **2006**, *5*, 107 – 115.
[17] J. E. T. Corrie, V. R. N. Munasinghe, D. R. Trentham, A. Barth, *Photochem. Photobiol. Sci.* **2008**, *7*, 84 – 97.
[18] J. D. Margerum, C. T. Petrusis, *J. Am. Chem. Soc.* **1969**, *91*, 2467 – 2472.
[19] K. Neumann, M.-K. Verhoefen, J.-M. Mewes, A. Dreuw, J. Wachtveitl, *Phys. Chem. Chem. Phys.* **2011**, *13*, 17367 – 17377.
[20] J.-M. Mewes, K. Neumann, M.-K. Verhoefen, G. Wille, J. Wachtveitl, A. Dreuw, *ChemPhysChem* **2011**, *12*, 2077 – 2080.
[21] R. L. Redington, *J. Phys. Chem.* **1976**, *80*, 229 – 235.
[22] B. H. Gibbons, J. T. Edsall, *J. Biol. Chem.* **1963**, *238*, 3502 – 3507.
[23] V. M. Krishnamurthy, G. K. Kaufman, A. R. Urbach, I. Gitlin, K. L. Gudiksen, D. B. Weibel, G. M. Whitesides, *Chem. Rev.* **2008**, *108*, 946 – 1051.
[24] W. W. Cleland, T. J. Andrews, S. Gutteridge, F. C. Hartman, G. H. Lorimer, *Chem. Rev.* **1998**, *98*, 549 – 562.
[25] E. Jabri, M. Carr, R. Hausinger, P. Karplus, *Science* **1995**, *268*, 998 – 1004.
[26] P. V. Attwood, J. C. Wallace, *Acc. Chem. Res.* **2002**, *35*, 113 – 120.
[27] G. Gros, H. S. Rollema, R. E. Forster, *J. Biol. Chem.* **1981**, *256*, 5471 – 5480.
[28] G. F. Versteeg, L. A. J. Van Dijck, W. P. M. Van Swaaij, *Chem. Eng. Commun.* **1996**, *144*, 113 – 158.
[29] E. F. da Silva, H. F. Svendsen, *Ind. Eng. Chem. Res.* **2006**, *45*, 2497 – 2504.
[30] W. A. Laing, J. T. Christeller, *Biochem. J.* **1976**, *159*, 563 – 570.
[31] G. H. Lorimer, M. R. Badger, T. J. Andrews, *Biochemistry* **1976**, *15*, 529 – 536.
[32] I. Andersson, S. Knight, G. Schneider, Y. Lindqvist, T. Lundqvist, C.-I. Brändén, G. H. Lorimer, *Nature* **1989**, *337*, 229 – 234.
[33] M. E. Salvucci, A. R. Portis, W. L. Ogren, *Anal. Biochem.* **1986**, *153*, 97 – 101.
[34] M. Kandel, A. G. Gornall, D. L. Cybulsky, S. I. Kandel, *J. Biol. Chem.* **1978**, *253*, 679 – 685.
[35] K. Izui, H. Matsumura, T. Furumoto, Y. Kai, *Annu. Rev. Plant. Biol.* **2004**, *55*, 69 – 84.
[36] T. Nakamura, I. Yoshioka, M. Takahashi, H. Toh, K. Izui, *J. Biochem.* **1995**, *118*, 319 – 324.
[37] A. Roth, F. Dornuf, O. Klein, D. Schneditz, H. Hafner-Gießauf, W. Mäntele, *Anal. Bioanal. Chem.* **2012**, *403*, 391 – 399.
[38] C. R. Somerville, S. C. Somerville, *Mol. Gen. Genet.* **1984**, *193*, 214 – 219.
[39] I. L. Norton, M. H. Welch, F. C. Hartman, *J. Biol. Chem.* **1975**, *250*, 8062 – 8068.
[40] K. Terada, T. Murata, K. Izui, *J. Biochem.* **1991**, *109*, 49 – 54.
[41] H. A. Staab, L. Schanne, C. Krieger, V. Taglieber, *Chem. Ber.* **1985**, *118*, 1204 – 1229.
[42] S. Ghorai, A. Bhattacharjya, A. Basak, A. Mitra, R. T. Williamson, *J. Org. Chem.* **2003**, *68*, 617 – 620.
[43] G. M. Sheldrick, *Acta Crystallogr. Sect. A Found Crystallogr.* **1990**, *46*, 467 – 473.
[44] G. M. Sheldrick, *Acta Crystallogr. Sect. A Found. Crystallogr.* **2008**, *64*, 112 – 122.
[45] J.-Y. Le Questel, M. Berthelot, C. Laurence, *J. Phys. Org. Chem.* **2000**, *13*, 347 – 358.

Received: October 15, 2012
Published online on January 16, 2013